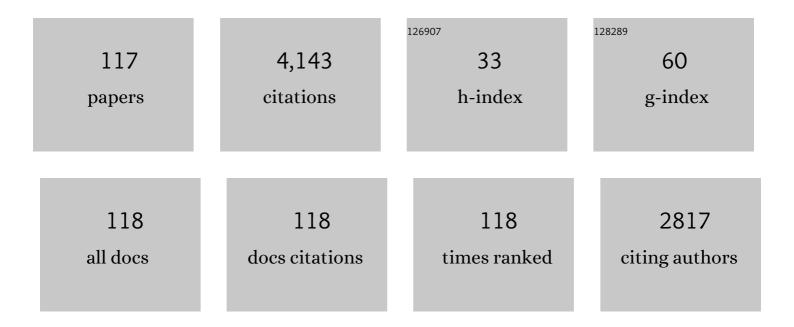
List of Publications by Year in descending order

Source: https://exaly.com/author-pdf/3203826/publications.pdf Version: 2024-02-01



SHI-KUAN SUN

| # | Article | IF | CITATIONS |
|----|--|------|-----------|
| 1 | Preparation and electrical properties of graphene nanosheet/Al2O3 composites. Carbon, 2010, 48, 1743-1749. | 10.3 | 315 |
| 2 | High Energy Storage Density and Large Strain in Bi(Zn _{2/3} Nb _{1/3})O ₃ -Doped BiFeO ₃ –BaTiO ₃ Ceramics. ACS Applied Energy Materials, 2018, 1, 4403-4412. | 5.1 | 229 |
| 3 | Mechanism of enhanced energy storage density in AgNbO3-based lead-free antiferroelectrics. Nano Energy, 2021, 79, 105423. | 16.0 | 180 |
| 4 | Dense high-entropy boride ceramics with ultra-high hardness. Scripta Materialia, 2019, 164, 135-139. | 5.2 | 177 |
| 5 | BiFeO ₃ -BaTiO ₃ : A new generation of lead-free electroceramics. Journal of Advanced Dielectrics, 2018, 08, 1830004. | 2.4 | 166 |
| 6 | Ultrahigh energy density in short-range tilted NBT-based lead-free multilayer ceramic capacitors by nanodomain percolation. Energy Storage Materials, 2021, 38, 113-120. | 18.0 | 139 |
| 7 | Structure-property relationships in manganese oxide - mesoporous silica nanoparticles used for T1-weighted MRI and simultaneous anti-cancer drug delivery. Biomaterials, 2012, 33, 2388-2398. | 11.4 | 135 |
| 8 | Novel BaTiO ₃ -Based, Ag/Pd-Compatible Lead-Free Relaxors with Superior Energy Storage Performance. ACS Applied Materials & Interfaces, 2020, 12, 43942-43949. | 8.0 | 130 |
| 9 | Microstructure and mechanical properties of high-entropy borides derived from boro/carbothermal reduction. Journal of the European Ceramic Society, 2019, 39, 3920-3924. | 5.7 | 127 |
| 10 | Fatigue resistant lead-free multilayer ceramic capacitors with ultrahigh energy density. Journal of Materials Chemistry A, 2020, 8, 11414-11423. | 10.3 | 114 |
| 11 | Perspectives on Working Voltage of Aqueous Supercapacitors. Small, 2022, 18, e2106360. | 10.0 | 93 |
| 12 | Chemical Reactions, Anisotropic Grain Growth and Sintering Mechanisms of Self-Reinforced ZrB2-SiC Doped with WC. Journal of the American Ceramic Society, 2011, 94, 1575-1583. | 3.8 | 91 |
| 13 | Dense and pure high-entropy metal diboride ceramics sintered from self-synthesized powders via boro/carbothermal reduction approach. Science China Materials, 2019, 62, 1898-1909. | 6.3 | 89 |
| 14 | Lead-free (Ba,Sr)TiO3 – BiFeO3 based multilayer ceramic capacitors with high energy density. Journal of the European Ceramic Society, 2020, 40, 1779-1783. | 5.7 | 79 |
| 15 | Low permittivity cordierite-based microwave dielectric ceramics for 5C/6G telecommunications. Journal of the European Ceramic Society, 2022, 42, 2820-2826. | 5.7 | 76 |
| 16 | Dielectric temperature stability and energy storage performance of NBTâ€based ceramics by introducing highâ€entropy oxide. Journal of the American Ceramic Society, 2022, 105, 4796-4804. | 3.8 | 73 |
| 17 | Ultra-low temperature co-fired ceramics with adjustable microwave dielectric properties in the Na ₂ O–Bi ₂ O ₃ –MoO ₃ 3study. Journal of Materials Chemistry C, 2022, 10, 2008-2016. | 5.5 | 65 |
| 18 | Ferroelectric Response Induced in <i>cis</i> -Type Anion Ordered SrTaO ₂ N Oxynitride Perovskite. Chemistry of Materials, 2016, 28, 1312-1317. | 6.7 | 61 |

| # | Article | IF | CITATIONS |
|----|--|------|-----------|
| 19 | Temperature stable Sm(Nb _{1â^'x} V _x)O ₄ (0.0 ≤i>x ≤0.9) microwave dielectric ceramics with ultra-low dielectric loss for dielectric resonator antenna applications. Journal of Materials Chemistry C, 2021, 9, 9962-9971. | 5.5 | 60 |
| 20 | Reactive spark plasma sintering of ZrC and HfC ceramics with fine microstructures. Scripta Materialia, 2013, 69, 139-142. | 5.2 | 59 |
| 21 | High-entropy A2B2O7-type oxide ceramics: A potential immobilising matrix for high-level radioactive waste. Journal of Hazardous Materials, 2021, 415, 125596. | 12.4 | 59 |
| 22 | Direct Integration of Cold Sintered, Temperature-Stable Bi2Mo2O9-K2MoO4 Ceramics on Printed Circuit Boards for Satellite Navigation Antennas. Journal of the European Ceramic Society, 2020, 40, 4029-4034. | 5.7 | 52 |
| 23 | Optimal preparation of high-entropy boride-silicon carbide ceramics. Journal of Advanced Ceramics, 2021, 10, 173-180. | 17.4 | 52 |
| 24 | Design of a Sub-6 GHz Dielectric Resonator Antenna with Novel Temperature-Stabilized (Sm _{1–<i>x</i>} Bi _{<i>x</i>})NbO ₄ (<i>x</i> = 0–0.15) Microwave Dielectric Ceramics. ACS Applied Materials & Interfaces, 2022, 14, 7030-7038. | 8.0 | 52 |
| 25 | Remarkably enhanced photocatalytic performance of Au/AgNbO3 heterostructures by coupling piezotronic with plasmonic effects. Nano Energy, 2022, 95, 107031. | 16.0 | 51 |
| 26 | Improved densification and hardness of high-entropy diboride ceramics from fine powders synthesized via borothermal reduction process. Ceramics International, 2020, 46, 14299-14303. | 4.8 | 49 |
| 27 | ZrO2 removing reactions of Groups IV–VI transition metal carbides in ZrB2 based composites. Journal of the European Ceramic Society, 2011, 31, 421-427. | 5.7 | 45 |
| 28 | Additive Sintering, Postannealing, and Dielectric Properties of <scp><scp>SrTaO</scp></scp> ₂ <scp>N</scp> . Journal of the American Ceramic Society, 2014, 97, 1023-1027. | 3.8 | 45 |
| 29 | Cold sintered LiMgPO ₄ based composites for low temperature coâ€fired ceramic (LTCC) applications. Journal of the American Ceramic Society, 2020, 103, 6237-6244. | 3.8 | 45 |
| 30 | Processing of dielectric oxynitride perovskites for powders, ceramics, compacts and thin films. Dalton Transactions, 2015, 44, 10570-10581. | 3.3 | 42 |
| 31 | Highâ€Temperature Flexible Nanocomposites with Ultraâ€High Energy Storage Density by Nanostructured MgO Fillers. Advanced Functional Materials, 2022, 32, . | 14.9 | 41 |
| 32 | Fabrication of textured (Hf0.2Zr0.2Ta0.2Cr0.2Ti0.2)B2 high-entropy ceramics. Journal of the European Ceramic Society, 2021, 41, 1015-1019. | 5.7 | 40 |
| 33 | 5G microstrip patch antenna and microwave dielectric properties of cold sintered LiWVO6–K2MoO4 composite ceramics. Ceramics International, 2021, 47, 19241-19246. | 4.8 | 37 |
| 34 | High Q×f values of Zn-Ni co-modified LiMg0.9Zn0.1-Ni PO4 microwave dielectric ceramics for 5G/6G LTCC modules. Journal of the European Ceramic Society, 2022, 42, 5684-5690. | 5.7 | 34 |
| 35 | Properties and microstructure of basic magnesium sulfate cement: Influence of silica fume. Construction and Building Materials, 2021, 266, 121076. | 7.2 | 33 |
| 36 | Microwave dielectric properties of Mg1.8R0.2Al4Si5O18 (R = Mg, Ca, Sr, Ba, Mn, Co, Ni, Cu, Zn) cordierite ceramics and their application for 5G microstrip patch antenna. Journal of the European Ceramic Society, 2022, 42, 2254-2260. | 5.7 | 33 |

| # | Article | IF | CITATIONS |
|----|---|-----|-----------|
| 37 | Highly Improved Microwave Absorbing and Mechanical Properties in Cold Sintered ZnO by Incorporating Graphene Oxide. Journal of the European Ceramic Society, 2022, 42, 993-1000. | 5.7 | 31 |
| 38 | Synthesis and characterisation of Ca1-xCexZrTi2-2xCr2xO7: Analogue zirconolite wasteform for the immobilisation of stockpiled UK plutonium. Journal of the European Ceramic Society, 2020, 40, 5909-5919. | 5.7 | 29 |
| 39 | Characterization of and Structural Insight into Struvite-K, MgKPO ₄ ·6H ₂ O, an Analogue of Struvite. Inorganic Chemistry, 2021, 60, 195-205. | 4.0 | 29 |
| 40 | Reactive spark plasma sintering of binderless WC ceramics at 1500°C. International Journal of Refractory Metals and Hard Materials, 2014, 43, 42-45. | 3.8 | 27 |
| 41 | Reactive spark plasma synthesis of CaZrTi2O7 zirconolite ceramics for plutonium disposition. Journal of Nuclear Materials, 2018, 500, 11-14. | 2.7 | 27 |
| 42 | A systematic investigation of the phase assemblage and microstructure of the zirconolite CaZr1-xCexTi2O7 system. Journal of Nuclear Materials, 2020, 535, 152137. | 2.7 | 26 |
| 43 | Additive sintering and post-ammonolysis of dielectric BaTaO2N oxynitride perovskite. Journal of the European Ceramic Society, 2016, 36, 3341-3345. | 5.7 | 25 |
| 44 | Review of zirconolite crystal chemistry and aqueous durability. Advances in Applied Ceramics, 2021, 120, 69-83. | 1.1 | 25 |
| 45 | New lowâ€ <i>ε_r</i> , temperature stable Mg ₃ B ₂ O ₆ â€Ba ₃ (VO ₄) ₂ microwave composite ceramic for 5G application. Journal of the American Ceramic Society, 2021, 104, 3818-3822. | 3.8 | 25 |
| 46 | Synergy of nanodiamond–doxorubicin conjugates and PD-L1 blockade effectively turns tumor-associated macrophages against tumor cells. Journal of Nanobiotechnology, 2021, 19, 268. | 9.1 | 25 |
| 47 | Nano-infiltration and transient eutectic (NITE) phase joining SiC ceramics at 1500oC. Ceramics International, 2019, 45, 24927-24931. | 4.8 | 24 |
| 48 | Texture, microstructures, and mechanical properties of AlNâ€based ceramics with Si ₃ N ₄ –Y ₂ O ₃ additives. Journal of the American Ceramic Society, 2017, 100, 3380-3384. | 3.8 | 23 |
| 49 | Direct synthesis of SrTaO2N from SrCO3/Ta3N5 involving CO evolution. Journal of the European Ceramic Society, 2014, 34, 4451-4455. | 5.7 | 22 |
| 50 | Fabrication of Nanosized Tungsten Carbide Ceramics by Reactive Spark Plasma Sintering. Journal of the American Ceramic Society, 2011, 94, 3230-3233. | 3.8 | 20 |
| 51 | Reaction Sintering of <scp><scp>HfC</scp></scp> <scp>W</scp> Cermets with High Strength and Toughness. Journal of the American Ceramic Society, 2013, 96, 867-872. | 3.8 | 19 |
| 52 | Structural evolution in ZrC-SiC composite irradiated by 4†MeV Au ions. Nuclear Instruments & Methods in Physics Research B, 2018, 434, 23-28. | 1.4 | 18 |
| 53 | Synthesis of single-phase metal oxycarbonitride ceramics. Scripta Materialia, 2020, 176, 17-22. | 5.2 | 18 |
| 54 | Bottom-up synthesis of 2D layered high-entropy transition metal hydroxides. Nanoscale Advances, 2022, 4, 2468-2478. | 4.6 | 17 |

| # | Article | IF | CITATIONS |
|----|---|------|-----------|
| 55 | Continuous and symmetric graded Si3N4 ceramics designed by spark plasma sintering at 15â€ [–] MPa. Ceramics International, 2019, 45, 16703-16706. | 4.8 | 16 |
| 56 | Improvement of densification and microstructure of HfB ₂ ceramics by Ta/Ti substitution for Hf. Journal of the American Ceramic Society, 2020, 103, 103-111. | 3.8 | 16 |
| 57 | High-Quality-Factor AlON Transparent Ceramics for 5 GHz Wi-Fi Aesthetically Decorative Antennas. ACS Applied Materials & Interfaces, 2021, 13, 46866-46874. | 8.0 | 16 |
| 58 | Direct synthesis of nearly single-phase BaTaO2N and CaTaO2N powders. Journal of the European Ceramic Society, 2015, 35, 3289-3294. | 5.7 | 15 |
| 59 | Reactive spark plasma sintering of Cs-exchanged chabazite: characterisation and durability assessment for Fukushima Daiichi NPP clean-up. Journal of Nuclear Science and Technology, 2019, 56, 891-901. | 1.3 | 15 |
| 60 | Pressureless joining of silicon carbide using Ti3SiC2 MAX phase at 1500oC. Ceramics International, 2020, 46, 14269-14272. | 4.8 | 15 |
| 61 | Sn4+ induced Bi3+ multi-lattice selective occupation and its color-tunable emission of La2MgZrO6: Bi3+, Sn4+ double perovskite phosphors. Journal of Alloys and Compounds, 2022, 902, 163724. | 5.5 | 15 |
| 62 | Synthesis mechanism and sintering behavior of tungsten carbide powder produced by a novel solid state reaction of W2N. International Journal of Refractory Metals and Hard Materials, 2012, 35, 202-206. | 3.8 | 13 |
| 63 | Particle refinement of ZrB ₂ by the combination of borothermal reduction and solid solution. Journal of the American Ceramic Society, 2017, 100, 524-528. | 3.8 | 13 |
| 64 | Effect of ZrB ₂ content on phase assemblage and mechanical properties of Si ₃ N ₄ –ZrB ₂ ceramics prepared at low temperature. Journal of the American Ceramic Society, 2018, 101, 4870-4875. | 3.8 | 13 |
| 65 | Selection principle of the synthetic route for fabrication of HfB ₂ and HfB ₂ â€ s iC ceramics. Journal of the American Ceramic Society, 2019, 102, 6427-6432. | 3.8 | 13 |
| 66 | Crystal and Electronic Structures of A ₂ NaIO ₆ Periodate Double Perovskites (A = Sr, Ca, Ba): Candidate Wasteforms for I-129 Immobilization. Inorganic Chemistry, 2020, 59, 18407-18419. | 4.0 | 13 |
| 67 | Powder synthesis, densification, microstructure and mechanical properties of Hf-based ternary boride ceramics. Journal of the European Ceramic Society, 2021, 41, 3922-3928. | 5.7 | 13 |
| 68 | A microexplosion method for the synthesis of graphene nanoribbons. Carbon, 2011, 49, 1439-1445. | 10.3 | 12 |
| 69 | High-temperature stability and densification of Ti-substituted ZrB2-based ceramics. Ceramics International, 2019, 45, 15749-15753. | 4.8 | 12 |
| 70 | Powder characteristics, sinterability, and mechanical properties of TiB ₂ prepared by three reduction methods. Journal of the American Ceramic Society, 2019, 102, 4511-4519. | 3.8 | 12 |
| 71 | Synthesis, structure, and characterization of the thorium zirconolite CaZr _{1â€x} Th _x Ti ₂ O ₇ system. Journal of the American Ceramic Society, 2021, 104, 2937-2951. | 3.8 | 12 |
| 72 | Lattice occupying sites and microwave dielectric properties of Mg2+–Si4+ co-doped MgxY3-xAl5-xSixO12 garnet typed ceramics. Journal of Materials Science: Materials in Electronics, 2022, 33, 2116-2124. | 2.2 | 12 |

| # | Article | IF | CITATIONS |
|----|---|------|-----------|
| 73 | Phase Evolution in the CaZrTi ₂ O ₇ –Dy ₂ Ti ₂ O ₇ System: A Potential Host Phase for Minor Actinide Immobilization. Inorganic Chemistry, 2022, 61, 5744-5756. | 4.0 | 12 |
| 74 | Ultraâ€Fine Tungsten Carbide Powder Prepared by a Nitridation–Carburization Method. Journal of the American Ceramic Society, 2010, 93, 3565-3568. | 3.8 | 11 |
| 75 | Pressureless joining of SiC ceramics at low temperature. Ceramics International, 2019, 45, 6556-6559. | 4.8 | 11 |
| 76 | Effects of the joining process on the microstructure and properties of liquid-phase-sintered SiC-SiC joints formed with Ti foil. Journal of the European Ceramic Society, 2021, 41, 225-232. | 5.7 | 11 |
| 77 | Crystal structure and microwave dielectric properties of Mg2+-Si4+ co-modified yttrium aluminum garnet ceramics. Journal of Materials Science: Materials in Electronics, 2022, 33, 4712-4720. | 2.2 | 11 |
| 78 | Graded Si3N4 ceramics with hard surface and tough core by two-step hot pressing. Ceramics International, 2017, 43, 7948-7950. | 4.8 | 10 |
| 79 | Lowâ€ŧemperature joining of SiC ceramics using NITE phase with Al 2 O 3 â€Ho 2 O 3 additive. Journal of the American Ceramic Society, 2020, 103, 731-736. | 3.8 | 10 |
| 80 | Conjugation with nanodiamonds via hydrazone bond fundamentally alters intracellular distribution and activity of doxorubicin. International Journal of Pharmaceutics, 2021, 606, 120872. | 5.2 | 10 |
| 81 | Preparation and oxidation behaviour of SiC-based ceramics with TaB2 addition. Ceramics International, 2019, 45, 23836-23840. | 4.8 | 9 |
| 82 | A new approach to the immobilisation of technetium and transuranics: Co-disposal in a zirconolite ceramic matrix. Journal of Nuclear Materials, 2020, 528, 151885. | 2.7 | 9 |
| 83 | Efficient toluene adsorption/desorption on biochar derived from in situ acid-treated sugarcane bagasse. Environmental Science and Pollution Research, 2021, 28, 62616-62627. | 5.3 | 9 |
| 84 | Lattices selective occupation, optical spectra regulation, and photoluminescence properties of Eu2+ activated Ca9La(PO4)7 phosphor. Journal of Luminescence, 2021, 237, 118197. | 3.1 | 9 |
| 85 | Nanoplates forced alignment of multi-walled carbon nanotubes in alumina composite with high strength and toughness. Journal of the European Ceramic Society, 2021, 41, 5541-5547. | 5.7 | 9 |
| 86 | Synthesis of perovskite BaTaO2N and SrNbO2N using TaN/NbN as the nitrogen source. Ceramics International, 2018, 44, 23324-23328. | 4.8 | 8 |
| 87 | Safely probing the chemistry of Chernobyl nuclear fuel using micro-focus X-ray analysis. Journal of Materials Chemistry A, 2021, 9, 12612-12622. | 10.3 | 8 |
| 88 | Influence of accessory phases and surrogate type on accelerated leaching of zirconolite wasteforms. Npj Materials Degradation, 2021, 5, . | 5.8 | 8 |
| 89 | Influence of TiB2 and CrB2 on densification, microstructure, and mechanical properties of ZrB2 ceramics. Ceramics International, 2021, 47, 28008-28013. | 4.8 | 8 |
| 90 | Synthesis of Ca1-xCexZrTi2-2xAl2xO7 zirconolite ceramics for plutonium disposition. Journal of Nuclear Materials, 2021, 556, 153198. | 2.7 | 8 |

| # | Article | IF | CITATIONS |
|-----|---|------|-----------|
| 91 | Significantly reduced conductivity in strontium titanate-based lead-free ceramics by excess bismuth. Materials Letters, 2022, 309, 131453. | 2.6 | 8 |
| 92 | Synthesis and characterisation of Ce-doped zirconolite Ca0.80Ce0.20ZrTi1.60M0.4007 (M = Fe, Al) formed by reactive spark plasma sintering (RSPS). MRS Advances, 2022, 7, 75-80. | 0.9 | 8 |
| 93 | Lead-free borosilicate glass/fused quartz composites for LTCC applications. Journal of Materials Science: Materials in Electronics, 2022, 33, 15033-15038. | 2.2 | 8 |
| 94 | Direct synthesis of nearly single phase SrTaO2N from SrCO3/TaN. Ceramics International, 2018, 44, 4504-4507. | 4.8 | 7 |
| 95 | Improvement of sinterability and mechanical properties of ZrB2 ceramics by the modified borothermal reduction methods. Journal of the European Ceramic Society, 2020, 40, 3844-3850. | 5.7 | 7 |
| 96 | Dense and coreâ€rim structured B 4 Câ€TiB 2 ceramics with Moâ€Coâ€WC additive. Journal of the American Ceramic Society, 2021, 104, 2860-2867. | 3.8 | 7 |
| 97 | Engineering lithiophilic Ni-Al@LDH interlayers on a garnet-type electrolyte for solid-state lithium metal batteries. Chemical Communications, 2021, 57, 10214-10217. | 4.1 | 7 |
| 98 | Hardness and toughness improvement of SiCâ€based ceramics with the addition of (Hf _{0.2} Mo _{0.2} Ta _{0.2} Nb _{0.2} Ti _{0.2} B ₂ . Journal of the American Ceramic Society, 2022, 105, 1629-1634. | 3.8 | 7 |
| 99 | Rapid synthesis of zirconolite ceramic wasteform by microwave sintering for disposition of plutonium. Journal of Nuclear Materials, 2020, 539, 152332. | 2.7 | 6 |
| 100 | Low-temperature catalytic combustion of benzene over Zr–Mn mixed oxides synthesized by redox-precipitation method. Journal of Materials Science, 2021, 56, 13540-13555. | 3.7 | 6 |
| 101 | Structure analysis of vitusite glass–ceramic waste forms using extended X-ray absorption fine structures. Ceramics International, 2017, 43, 4687-4691. | 4.8 | 5 |
| 102 | Effect of CeO ₂ and Al ₂ O ₃ contents on Ceâ€ZrO ₂ /Al ₂ O ₃ composites. Journal of the American Ceramic Society, 2018, 101, 2066-2073. | 3.8 | 5 |
| 103 | Temperature Stable, High-Quality Factor Li2TiO3-Li4NbO4F Microwave Dielectric Ceramics. Crystals, 2021, 11, 741. | 2.2 | 5 |
| 104 | Dense SiC ceramics prepared by using amorphous sintering additives. Ceramics International, 2022, 48, 16449-16454. | 4.8 | 5 |
| 105 | Effect of native carbon vacancies on evolution of defects in ZrC1- under He ion irradiation and annealing. Journal of Materials Science and Technology, 2022, 119, 87-97. | 10.7 | 5 |
| 106 | Preparation and luminescence properties of Eu2+-doped oxynitride feldspar SrAl2â^'Si2+O8â^'N. Journal of Alloys and Compounds, 2015, 618, 254-257. | 5.5 | 4 |
| 107 | On the existence of the compound "Ce3NbO7+―prepared under air atmosphere. Journal of Rare Earths, 2021, 39, 596-599. | 4.8 | 4 |
| 108 | Core-Shell Structure and Dielectric Properties of Ba0.6Sr0.4TiO3@ Fe2O3 Ceramics Prepared by Co-Precipitation Method. Crystals, 2021, 11, 623. | 2.2 | 4 |

| # | Article | IF | CITATIONS |
|-----|--|-----|-----------|
| 109 | Chemical state mapping of simulant Chernobyl lava-like fuel containing material using micro-focused synchrotron X-ray spectroscopy. Journal of Synchrotron Radiation, 2021, 28, 1672-1683. | 2.4 | 4 |
| 110 | Synthesis and characterisation of HIP Ca0.80Ce0.20ZrTi1.60Cr0.40O7 zirconolite and observations of the ceramic–canister interface. MRS Advances, 2021, 6, 112-118. | 0.9 | 3 |
| 111 | Low-Temperature Nitridation of Fe ₃ O ₄ by Reaction with NaNH ₂ . Inorganic Chemistry, 2021, 60, 2553-2562. | 4.0 | 3 |
| 112 | Chemical characterisation of degraded nuclear fuel analogues simulating the Fukushima Daiichi nuclear accident. Npj Materials Degradation, 2022, 6, . | 5.8 | 3 |
| 113 | Microstructure evolution of MeB2 (Me=Zr, Ti) powders prepared by borothermal reduction during heat treatment at 1000°C–1800°C. Ceramics International, 2019, 45, 23794-23797. | 4.8 | 2 |
| 114 | Low-temperature joining of silicon carbide via Al-air in situ reaction. Ceramics International, 2019, 45, 24932-24935. | 4.8 | 1 |
| 115 | Synthesis of zirconolite-2M ceramics for immobilisation of neptunium. Ceramics International, 2021, 47, 1047-1052. | 4.8 | 1 |
| 116 | Ceramic-based stabilization/solidification of radioactive waste. , 2022, , 449-468. | | 1 |
| 117 | Temperature-dependent discharge performance of (Pb0.87Ba0.08Sr0.02La0.02) (Zr0.65Sn0.27Ti0.08) O3 antiferroelectric ceramics. Journal of Materials Science: Materials in Electronics, 2022, 33, 5468. | 2.2 | 1 |